anchoring mechanism and provides a nucleation site for further atoms. And, perhaps most importantly, the SMAD method allows versatility in preparing bimetallic catalyst particles, sometimes in layered structures and sometimes as alloy-like particles. Such novel bimetallic small particles would be difficult if not impossible to prepare by conventional synthetic schemes.

Articles

Decomposition Mechanisms of Trimethylantimony and Reactions with Trimethylindium

C. A. Larsen, S. H. Li, and G. B. Stringfellow*

Department of Materials Science and Engineering, University of Utah, Salt Lake City, Utah 84112

The decomposition of trimethylantimony (TMSb) was studied in a flow tube apparatus by using a variety of carrier gases and a mass spectrometer to analyze the products. Radical sources and scavengers were added to elucidate the mechanisms. In He, the main reactions are postulated to be a reversible homolytic scission of the first Sb–CH₃ bond followed by well-known radical reactions. This conclusion was supported by adding $(CH_3N)_2$ as a source of CH_3 groups: The effect was to retard the decomposition rate. Abstraction of H from TMSb apparently does not occur. In D_2 (H_2) the pyrolysis occurs at much lower temperatures than in He. A chain reaction is postulated in which CH_3 radicals react with the ambient to give D (H), which then reacts with TMSb to give CH_3D (CH_4) and additional CH_3. The existence of both CH_3 and D is shown by the products when toluene is added. The addition of trimethylindium (TMIn) results in lower decomposition temperatures for TMSb. The effect of TMIn is only indirect, with TMIn acting as a generator of D atoms (via reaction of CH_3 radicals with the D_2 ambient), which then accelerate TMSb decomposition. The presence of TMSb retards TMIn pyrolysis, presumably by depleting the concentration of D atoms, which are known to accelerate TMIn pyrolysis.
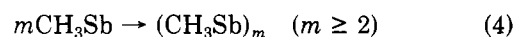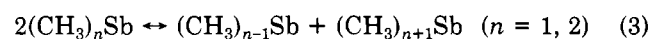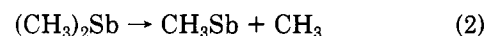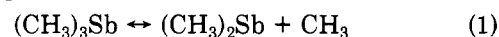
Introduction

Trimethylantimony (TMSb) is a well-known precursor for growth of group III/V semiconductors. It has been used successfully to produce the binary compounds GaSb[1,2] and InSb[3,4] as well as the ternary alloys InAsSb,[3,5] GaAsSb,[6] GaPSb,[7] and InPSb[8] and the quaternary alloys GaInAsSb[9] and InAsSbBi.[10] One of the surprising results

from using OMVPE (organometallic vapor-phase epitaxy) has been in the ability to grow novel alloys such as GaAsSb, GaPSb, InPSb, GaInAsSb, and InAsSbBi. The large difference in atomic radii between As or P and Sb results in miscibility gaps at OMVPE growth temperatures. Nevertheless, it is possible to grow these materials over the entire composition range. In general, OMVPE growth with TMSb seems to be a remarkably useful method for achieving compositions that cannot be obtained in other ways.

Investigations of the pyrolysis mechanisms of TMSb serve as a useful complement to the growth studies listed above. Immediate questions include the role of carrier gases and the effects of surfaces. Studies of the combined TMIn–TMSb system have direct relevance to the actual growth process. An improved understanding of the elementary steps in the decomposition has several practical applications, including a more realistic basis for numerical models of OMVPE growth. These studies may also assist with the development of other Sb precursors for special requirements such as lower growth temperatures.

Previous Studies of TMSb Decomposition

To date only four papers have been published on TMSb decomposition. In 1958, Price and Trotman-Dickenson[11] reported on the pyrolysis in a toluene carrier. The results were somewhat confusing and ambiguous. In a later paper[12] it was reported that some of the conclusions in ref 11 were erroneous. The second study postulated the main steps in the process to be

$$(CH_3)_3Sb \leftrightarrow (CH_3)_2Sb + CH_3 \qquad (1)$$

$$(CH_3)_2Sb \rightarrow CH_3Sb + CH_3 \qquad (2)$$

$$2(CH_3)_nSb \leftrightarrow (CH_3)_{n-1}Sb + (CH_3)_{n+1}Sb \quad (n = 1, 2) \qquad (3)$$

$$mCH_3Sb \rightarrow (CH_3Sb)_m \quad (m \geq 2) \qquad (4)$$

(1) Manasevit, H. M.; Hess, K. L. *J. Electrochem. Soc.* **1979**, *126*, 2031.
(2) Cooper, C. B.; Saxena, R. R.; Ludowise, M. J. *J. Electron. Mater.* **1982**, *11*, 1001.
(3) Biefeld, R. M. *J. Cryst. Growth* **1986**, *75*, 255.
(4) Chaing, P. K.; Bedair, S. M. *J. Electrochem. Soc.* **1984**, *131*, 2422.
(5) Jen, H. R.; Ma, K. Y.; Stringfellow, G. B. *Appl. Phys. Lett.* **1989**, *54*, 1154.
(6) Cherng, M. J.; Cherng, Y. T.; Jen, H. R.; Harper, P.; Cohen, R. M.; Stringfellow, G. B. *J. Electron. Mater.* **1986**, *15*, 79.
(7) Jou, M. J.; Cherng, Y. T.; Jen, H. R.; Stringfellow, G. B. *Appl. Phys. Lett.* **1988**, *52*, 549.
(8) Jou, M. J.; Cherng, Y. T.; Stringfellow, G. B. *Appl. Phys. Lett.* **1988**, *64*, 1472.

(9) Cherng, M. J.; Jen, H. R.; Larsen, C. A.; Stringfellow, G. B.; Lundt, H.; Taylor, P. C. *J. Cryst. Growth* **1986**, *77*, 408.
(10) Ma, K. Y.; Fang, Z. M.; Jaw, D. H.; Cohen, R. M.; Stringfellow, G. B.; Kosar, W. P.; Brown, D. W. *Appl. Phys. Lett.* **1989**, *55*, 2420.
(11) Price, S. J. W.; Trotman-Dickenson, A. F. *Trans. Faraday Soc.* **1958**, *54*, 1630.
(12) Price, S. J. W.; Richard, J. P. *Can. J. Chem.* **1972**, *50*, 966.

The reversibility of step 1 was determined in two ways. First, the rate constant for pyrolysis was found to increase with increasing toluene concentration. Toluene serves as a scavenger for methyl radicals; hence, by removing the radicals the decomposition rate was enhanced. Second, extensive isotopic mixing was observed for mixtures of $(CH_3)_3Sb$ and $(CD_3)_3Sb$. Recombination of methyl groups (CH_3 or CD_3) with unsaturated methylantimony fragments, as in the reverse reaction of step 1 (termed reaction -1 throughout this paper for simplicity of notation), is an efficient method of achieving this scrambling. In the first paper[11] reaction 3 was suggested, with $n = 2$, to explain the effect of toluene concentration on the rate constant. This reaction also results in isotopic mixing. It was not possible in the later study to rule out this process. Simple bond strength calculations and assumptions about preexponential factors in the Arrhenius equation (or A factors) indicated that step 3 with $n = 1$ was the most likely candidate for final production of antimony metal, rather than the expected homolytic scission of the third $Sb-CH_3$ bond. The last reaction was proposed to account for a buildup of small amounts of carbonaceous deposits in the reactor.

Under conditions where reaction -1 was suppressed, the rate constant for release of the first methyl group was determined to be

$$\log k_1 \ (s^{-1}) = 15.33 - 55.9 \pm 1 \ (\text{kcal/mol})/2.303RT \quad (5)$$

The toluene concentration at which this occurred was determined by noting the variation of rate constant with P_{toluene}, and the result was confirmed by the lack of any isotopic mixing above the critical concentration. The rate constant for step 2 was not determined. It is probably much faster than release of the first methyl group.

Travkin et al.[13] used a combination of differential thermal analysis and electrical conductivity measurements to observe the boiling point and the onset of decomposition of neat TMSb. The latter process occurred at 455 °C, as shown by an exothermic temperature effect and a sharp increase in the conductivity of the sample. However, even at temperatures as low as the boiling point (80 °C), some decomposition products were observed. These included methane, ethane, and ethene. The observation of pyrolysis at extremely low temperatures is important for explaining the present experimental results. Finally, the most recent study[9] indicated that an increase in SiO_2 surface area had little effect on the pyrolysis rate but that addition of powdered GaP greatly enhanced the decomposition. These conclusions may not be justified, because TMSb pyrolysis leaves a coating of Sb metal on all surfaces, rendering them all alike. This work investigates these phenomena in more detail.

Experimental Section

The apparatus used in these experiments has been described in detail elsewhere.[14] The carrier gases pass through mass flow controllers and then through PTFE–coated stainless steel bubblers containing the reactants. The gas mixture enters the "ersatz" reactor, which is a quartz tube of 4-mm i.d. and an isothermal hot zone 41.5 cm long. The exhaust gases are sampled continuously via a variable leak connected to a CVC 2000 time-of-flight mass spectrometer. The flow rate for all experiments involving the open tube was 40 sccm. The TMSb concentration for all experiments was 1%, or 6.35 Torr. In each case the reactor was conditioned by heating the tube to a temperature near which 50% of the TMSb decomposed. In some runs the tube was packed
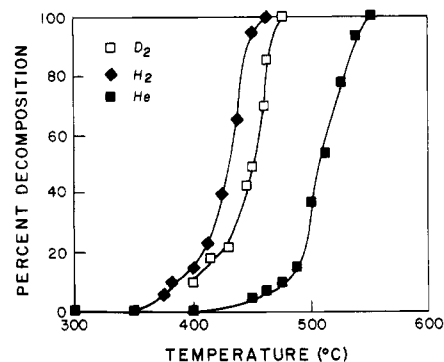
(13) Travkin, N. N.; Skachkov, B. K.; Tonoyan, I. G.; Kozyrkin, B. I. *J. Gen. Chem. USSR* 1978, *48*, 2428.

(14) Larsen, C. A.; Buchan, N. I.; Li, S. H.; Stringfellow, G. B. *J. Cryst. Growth* 1989, *94*, 663.

Figure 1. Pyrolysis of TMSb vs temperature and carrier gas. The concentration for all experiments was 1% (6.35 Torr).
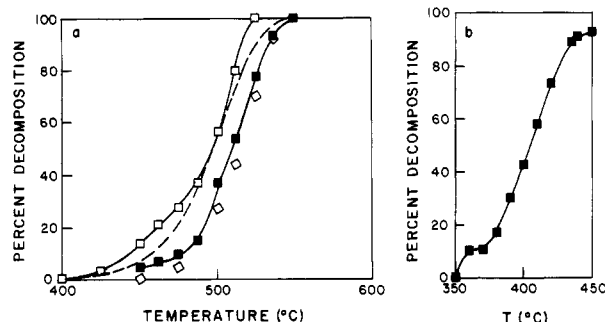

Figure 2. (a) Pyrolysis of TMSb (6.35 Torr) in He: ■, TMSb alone; □, with increased surface area; ◇, with added azomethane (6.35 Torr). Dashed curve is calculated from the data of ref 12. (b) Pyrolysis vs temperature for azomethane.

with SiO_2 chips to increase the surface area approximately 24 times. The flow rates were correspondingly adjusted to give the same residence times as for the unpacked runs. In some experiments toluene was added as a radical scavenger.

The TMSb was from Alfa Products division of Morton Thiokol. The toluene was from J. T. Baker Chemical Co. The azomethane was synthesized by the method of Foster and Beauchamp[15] using 1,2-dimethylhydrazine dihydrochloride purchased from Aldrich Chemical Co. The D_2 was research grade (to minimize background HD levels), from Air Products and Chemicals, Inc.

Results

Figure 1 shows the pyrolysis of TMSb (1%) vs temperature as a function of carrier gas. A definite effect is observed, the difference between He and D_2 being especially large. The error limits lead to an uncertainty in the data of ±5 °C. Carrier gas phenomena are common in main-group organometallic decomposition, but because of the wide range of chemical properties found in this small group of elements the causes of ambient effects may be quite different for neighboring elements. In the following section, further experiments in each of the carriers will be discussed. The results allow the main features of the decomposition mechanisms to be deduced.

Figure 2a gives the result of several experiments in He. The filled squares are reproduced from Figure 1. The open squares are for the packed tube, where the surface area is increased by a factor of 24, and demonstrate a slight surface effect. Since all surfaces are coated with Sb, the effect is autocatalytic.

The dashed line in Figure 2a is calculated from eq 5 for the residence times of our apparatus. This curve lies at lower temperatures than for TMSb alone, as expected on the basis of the rate-enhancing effect of the radical scavenger. Toluene was not used in the He experiments be-

(15) Foster, M. S.; Beauchamp, J. L. *J. Am. Chem. Soc.* 1972, *94*, 2425.

Trimethylantimony Decomposition and Reactions
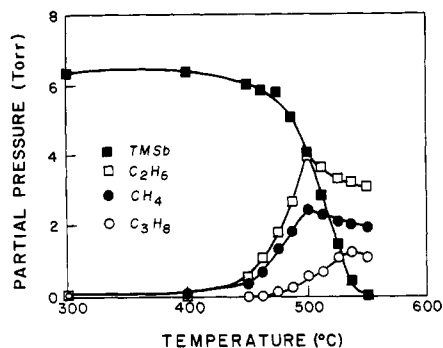
Chem. Mater., Vol. 3, No. 1, 1991 41

Figure 3. Products of TMSb decomposition in He. C_2H_6 and C_3H_8 data points include other C_2 and C_3 hydrocarbons.

cause the maximum toluene concentration, obtained by flowing the entire volume of carrier gas through the toluene bubbler held at room temperature, was 2.5%. This is below the concentration needed to observe an effect on the decomposition rate due to methyl radical capture, according to ref 12. However, Figure 2a shows that addition of 1% of azomethane in He slightly retards the decomposition. Azomethane $(CH_3N:NCH_3)$ serves as a "clean" source of methyl radicals, yielding mainly CH_3 and inert N_2.[16] Its pyrolysis curve is shown in Figure 2b for reference. The result with azomethane, together with the previously reported[12] data in toluene, are consistent with the proposal that step 1 is highly reversible.

Another possibility is the reverse of step 3. This could account for the isotopic mixing in ref 12 and (for $n = 2$) would retard TMSb pyrolysis. However, the experiments described in this paper clearly show that methyl radicals play an important role in the process.

The products in He are given in Figure 3. They include mainly C_2H_6, CH_4, and C_3H_8. Some C_2H_4 and C_3H_6 may have been formed, but their mass spectra are difficult to separate from the corresponding alkanes. These products can be explained by normal radical processes. The reactions may be complex, including methyl radical recombination to form ethane and the two-step process given in eqs 6 and 7 to produce propane. As with other free-radical

$$CH_3 + C_2H_6 \rightarrow CH_4 + C_2H_5 \qquad (6)$$

$$CH_3 + C_2H_5 \rightarrow C_3H_8 \qquad (7)$$
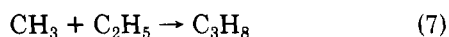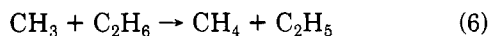
mechanisms, the entire list of possible steps is quite long.

Step 6, along with analogous reactions involving other hydrocarbons, produces the CH_4. Abstraction of H from the parent TMSb could also account for some of the CH_4. However, the fact that added CH_3 tends to retard the decomposition implies that the abstraction process is not a major reaction. Li et al.[17] reported that added CH_3 groups have little effect on the decomposition of another group 5 compound, trimethylarsine. In contrast, abstraction is one of the main steps in pyrolysis of trimethylgallium (TMGa).[18] The reasons for the differences between group III and group V compounds can be seen by reference to the molecular orbital structure of $(CH_3)_3M$ species with M = Ga or Sb. Before removal of an H atom, the CH_3 ligands attached to the M atom have sp^3 hybridization, and all orbitals connected to C are bonding ones. Dehydrogenation produces a CH_2 ligand with sp^2
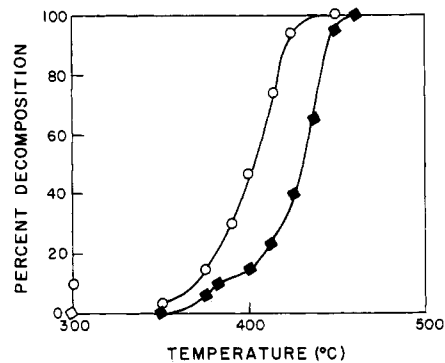
(16) Page, M.; Pritchard, H. O.; Trotman-Dickenson, A. F. *J. Chem. Soc.* **1953**, 3878.

(17) Li, S. H.; Larsen, C. A.; Stringfellow, G. B. *J. Cryst. Growth* **1990**, *102*, 117.

(18) Larsen, C. A.; Buchan, N. I.; Li, S. H.; Stringfellow, G. B. *J. Cryst. Growth* **1990**, *102*, 103.

Figure 4. Pyrolysis of 6.35 Torr of TMSb in H_2 with low ($\blacklozenge$) and high (O) surface areas.
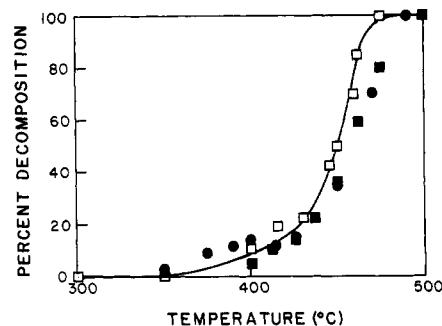

Figure 5. Pyrolysis of TMSb in D_2. $\square$, TMSb alone; $\bullet$, with 1% azomethane; $\blacksquare$, with 2.5% toluene.
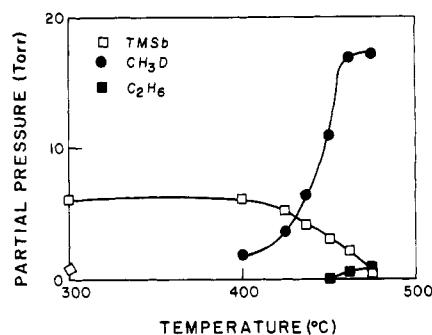

Figure 6. Products of TMSb pyrolysis in D_2.

hybridization and a half-filled p-like orbital on the central carbon atom. The empty nonbonding orbital on the Ga atom of TMGa has the same symmetry as the orbital on the CH_2 group, and the two can mix, thereby lowering the activation energy for removal of the H atom. With group V elements this mixing is not possible for two reasons. First, all orbitals on the central atom are filled. Second, the sp^3 hybridization of these orbitals does not allow overlap with the sp^2 orbital on the ligand. Thus abstraction from group V molecules is not favored, by simple stereochemical arguments.

Figure 4 is a plot of the pyrolysis of TMSb in H_2 with high and low surface areas. The effect is larger than for the He experiments. This phenomenon was not investigated further, and the discussion is limited to the gas-phase processes.

More information about the gas-phase chemistry is found by reference to Figure 5, which shows the pyrolysis behavior in D_2. The filled squares are from Figure 1. Addition of 1% azomethane retards the reaction slightly, similar to the results in He. Toluene also has a hindering effect, unlike the results reported in ref 12 in He. For the free radical scavenger, as well as the source, the effect is small.

Figure 7. Products of 1% TMSb pyrolysis in D_2 with toluene (2.5%). EtBz is ethylbenzene.

The products of the decomposition in D_2 are shown in Figure 6. The major product is CH_3D, with a trace of C_2H_6. No CH_4 could be detected. This is further evidence that attack by CH_3 on the parent TMSb or its decomposition products to abstract H atoms 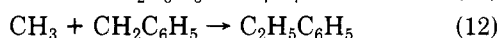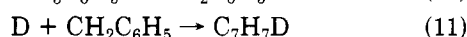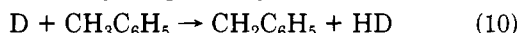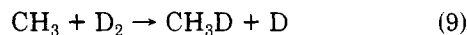is unimportant. No deuterated antimony species were found. The presence of C_2H_6 shows that free radicals are generated as part of the decomposition. The difference in C_2H_6 production in He vs D_2 can be explained in terms of the concentration dependence of the reaction. Recombination of CH_3 radicals is a second-order process and thus is highly sensitive to the CH_3 concentration. The large amount of ethane in the He experiments indicates that the concentration of CH_3 is high, while in D_2 the steady-state CH_3 concentration is low due to reactions with the ambient.

Figure 7 displays the products for the experiment in D_2 with 2.5% toluene. This concentration of toluene is not enough to completely suppress radical interactions. Nevertheless, important information was obtained from the product distribution. In this mixture the possible reactions include

$$CH_3 + CH_3C_6H_5 \rightarrow CH_4 + CH_2C_6H_5 \qquad (8)$$

$$CH_3 + D_2 \rightarrow CH_3D + D \qquad (9)$$

$$D + CH_3C_6H_5 \rightarrow CH_2C_6H_5 + HD \qquad (10)$$

$$D + CH_2C_6H_5 \rightarrow C_7H_7D \qquad (11)$$

$$CH_3 + CH_2C_6H_5 \rightarrow C_2H_5C_6H_5 \qquad (12)$$

$$2CH_3 \rightarrow C_2H_6 \qquad (13)$$

$$2CH_2C_6H_5 \rightarrow (CH_2C_6H_5)_2 \qquad (14)$$
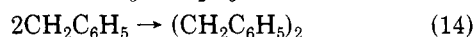
and other standard radical reactions. Reference to Figure 7 shows that no CH_4 is formed, so step 8 is slow. The HD can come only from reaction 10. Hence, some D atoms are present in the reacting mixture. By extension, reaction 9 must also be occurring to form the atomic species.

The slow rate of formation of CH_4, in spite of the presence of methyl radicals, is due merely to the competing kinetics of the various steps. The rate constant for step 8 is[19]

$$\log k_8 \ (L \ mol^{-1} \ s^{-1}) = 8.5 - 9.5 \ (kcal/mol)/2.303RT \qquad (15)$$

and for step 10[19]

$$\log k_{10} \ (L \ mol^{-1} \ s^{-1}) = 10.91 - 9.2 \ (kcal/mol)/2.303RT \qquad (16)$$

The relative rates of steps 8 and 10 are then

$$R_8/R_{10} = k_8[CH_3]/k_{10}[D] \qquad (17)$$

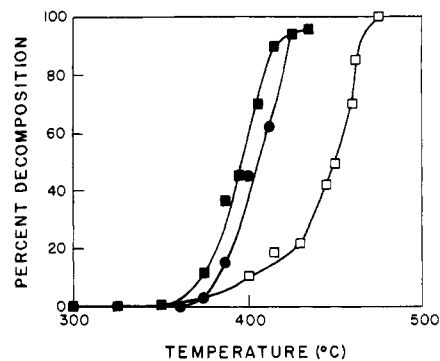The concentrations of CH_3 and D in the reactor can be estimated by considering steps 1 and 2 to generate CH_3,

Figure 8. Pyrolysis of 1% TMSb in D_2 alone (□) and with 1% TMIn at low (●) and high (■) surface areas.

followed by reactions 8–10. By combining the rate laws for this set of reactions and assuming steady-state conditions, the concentrations of the two radical species are given by

$$[CH_3] = 2k_1[TMSb]/(k_8[tol] + k_9[D_2]) \qquad (18)$$

$$[D] = k_9[CH_3][D_2]/k_{10}[tol] \qquad (19)$$

The concentration of D_2 is essentially constant. The concentrations of TMSb and toluene change with distance along the reactor tube, of course. The present calculations were done by assuming one-half the input concentration for TMSb (to give an average) and 2.5% toluene, to provide a "best case" for radical attack. At 450 °C the concentrations of methyls and D atoms are 1.42×10^{-9} and 7.53×10^{-11} mol/L. Upon substitution of these values into eq 17, $R_8/R_{10} = 5.94 \times 10^{-2}$. Thus methyl radical attack on toluene is unlikely.

The remaining products are accounted for by the reactions listed. Recombination of benzyl and methyl radicals would be essentially collision controlled, producing the ethylbenzene. The deuterated toluene is formed by reaction 11. Ethane is not reported in the figure. Its maximum concentration was approximately 0.1 Torr. No styrene or dibenzyl was detected.

A final point regarding the products is that in every case described above, a small amount of black material that did not dissolve in aqua regia was deposited on the reactor surfaces. Thus, it appears that reaction 4 takes place under these conditions as well. The carbonaceous material was not found when TMIn was added.

The last set of experiments to be described are those in which TMIn was added during TMSb pyrolysis. Figure 8 shows the pyrolysis of TMSb in D_2 alone (open squares, reproduced from Figure 1) and with TMIn. The concentrations of both reagents were nominally 1%. Data for the combined system are shown at high and low surface areas. Two features of the data should be noted. First, TMIn has a large accelerating effect on the decomposition of TMSb. The difference is almost as great as for the change on going from He to D_2. Second, the effect of surface area is minimal. This means that the process is largely homogeneous. More clues to the mechanism are found in the behavior of TMIn. At 350 °C, 32% of the TMIn had decomposed, whereas TMIn alone is approximately 70% pyrolyzed under similar conditions.[20] Thus TMSb retards the pyrolysis of TMIn. Finally, the main product for the TMIn–TMSb mixture is CH_3D, with a small amount of C_2H_6. No other products could be detected. These are the same compounds that are found for independent de-

(19) *CRC Handbook of Bimolecular and Termolecular Gas Reactions*; Kerr, J. A., Moss, S. J., Eds.; CRC Press: Boca Raton, FL, 1981.

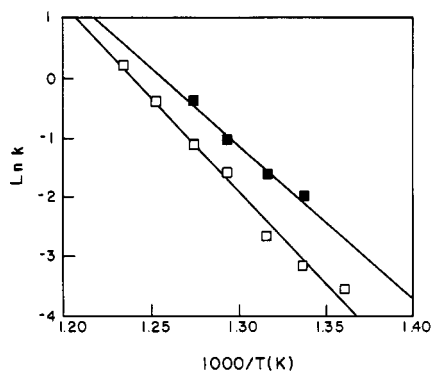(20) Buchan, N. I.; Larsen, C. A.; Stringfellow, G. B. *J. Cryst. Growth* **1988**, *92*, 591.

Figure 9. Arrhenius plots from decomposition curves of TMSb in He at low (□) and high (◆) surface areas.

composition of the two components.[20] A concerted pathway, such as adduct elimination, would produce mainly C_2H_6.

Discussion

The data presented above give enough information to formulate the major features of a mechanism of TMSb decomposition. First, the process is largely homogeneous. For a completely heterogeneous reaction, a 24-fold increase in the surface area should increase the experimental A factor by the same amount. Arrhenius plots of the decomposition in He at high and low surface areas (hsa and lsa, respectively) are shown in Figure 9, assuming first-order kinetics. The rate constants derived from the plots are
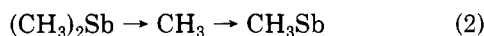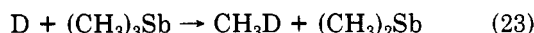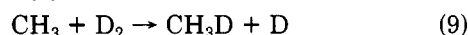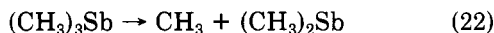
$$\log k_{lsa} \ (s^{-1}) = 16.86 - 62.3 \ (kcal/mol)/2.303RT \quad (20)$$

$$\log k_{hsa} \ (s^{-1}) = 14.21 - 51.57 \ (kcal/mol)/2.303RT \quad (21)$$

The preexponential factor is not a linear function of the surface area. Also, the difference in activation energies does not suggest a strong contribution from the surface reaction.

In He, then, the decomposition is dominated by reactions 1–4. The effects of azomethane and toluene[12] and the products are all consistent with this mechanism. The lack of any CH_4 in the D_2 ambient offers further evidence that the methyl radicals do not abstract H atoms from TMSb. Thus, simple homolytic fission followed by normal radical reactions appears to describe essentially all the features of the pyrolysis in an inert ambient.

In H_2 or D_2, the situation is somewhat more complex. The dashed curve in Figure 2a would seem to define the minimum temperature for release of methyl radicals as approximately 400 °C. In D_2 and H_2, however, the data in Figure 5 indicate that pyrolysis is already underway at this temperature. Furthermore, the product data in Figure 7 show clear evidence for free methyl radicals and D atoms. This is consistent with the findings of Travkin et al.[13] that hydrocarbons were produced from TMSb even at its boiling point, but that much higher temperatures were required to observe any decomposition. It appears that a small concentration of free radicals is present at the low temperatures, and it may be surmised that they are responsible for the enhanced pyrolysis. A chain reaction is thus indicated:

$$(CH_3)_3Sb \rightarrow CH_3 + (CH_3)_2Sb \quad (22)$$

$$CH_3 + D_2 \rightarrow CH_3D + D \quad (9)$$

$$D + (CH_3)_3Sb \rightarrow CH_3D + (CH_3)_2Sb \quad (23)$$

$$(CH_3)_2Sb \rightarrow CH_3 \rightarrow CH_3Sb \quad (2)$$

As mentioned above, step 2 is a rapid reaction. Studies

of TMGa[17] and dimethylmercury[21] have suggested that the steps analogous to (23) and (2) occur simultaneously for those compounds. It is not possible kinetically to distinguish between a one-step process and a two-step reaction in which the second reaction is fast.

The effects of TMIn are somewhat unexpected. For many III/V combinations, such as $TMIn/PH_3$[22] and trimethylgallium/AsH_3,[23] the decomposition of the two components occurs simultaneously, and the kinetic and product data indicate a concerted mechanism. For the TMGa/TBP (*tert*-butylphosphine) system, simultaneous decomposition enhances the rate of pyrolysis of TMGa and retards that of TBP,[24] the opposite of our obsevations for TMIn and TMSb. For TMGa/TBP the cause is competition for PH_2 radicals, which enhance the pyrolysis rates for both precursors. In the TMIn/TMSb case the cause is similar. The decomposition of the two species is largely independent, but both rates are enhanced by D atoms. It is convenient to conceive of the pyrolysis as occurring in two parts. The first step is homolytic fission of TMIn, forming two methyl groups.[25] It has been shown[20] that the next step in TMIn pyrolysis is attack on TMIn by D atoms, formed via reaction 9. TMSb competes for the D atoms (step 23). The net effect is a retardation of TMIn pyrolysis and a simultaneous increase in the decomposition rate of TMSb. Of course, the CH_3 radicals produced could also lead to the back reaction of step 1, which would reduce the net TMSb pyrolysis rate. At low temperatures, the effect of TMIn on the TMSb pyrolysis rate is mainly due to production of D.

An apparent dichotomy is that TMIn and azomethane both act as CH_3 sources, yet they have opposite effects on the TMSb pyrolysis rate. This can be understood by noting the difference in decomposition temperatures of TMIn and azomethane. As shown in Figure 2a, azomethane generates the methyl radicals at temperatures close to those at which TMSb pyrolyzes by itself. Thus while reaction 9 occurs to some extent, followed by step 23, so does reaction −1. In fact, the competition between these two processes probably accounts for the minimal shift in decomposition temperature when the azomethane is added in D_2. Similarly, the addition of toluene has two opposing effects on the TMSb pyrolysis rate. It removes both D atoms (to form $C_6H_5CH_2D$) and methyl radicals (to give ethylbenzene). The initial stages of TMIn pyrolysis, on the other hand, occur at much lower temperatures than for TMSb.[20] In our apparatus, most of the TMIn eliminates CH_3 radicals in the inlet portion of the reactor, before any TMSb is able to pyrolyze. Since there is no $(CH_3)_2Sb$ to scavenge the radicals, the CH_3 radicals have ample time to react with D_2 molecules. The resulting D causes a net increase in the TMSb pyrolysis rate.

Experiments with trimethylarsine[17] showed that a major product in D_2 is $(CH_3)_2AsD$ in addition to the CH_3D. The data indicated that the pyrolysis of that compound may proceed via hydrogenolysis, with a five-center transition state formed by addition of D_2 to the central atom. This leads to simultaneous formation of CH_3D and $(CH_3)_2AsD$. The thermodynamic data available indicate that this route is not likely for TMSb. Table I lists the best literature values for the bond strengths for ML_3, where M = As or

(21) Harris, G. M.; Steacie, E. W. R. *J. Chem. Phys.* **1945**, *13*, 559.

(22) Buchan, N. I.; Larsen, C. A.; Stringfellow, G. B. *J. Cryst. Growth* **1988**, *92*, 605.

(23) Larsen, C. A.; Li, S. H.; Buchan, N. I.; Stringfellow, G. B.; Brown, D. W. *J. Cryst. Growth* **1990**, *102*, 126.

(24) Li, S. H.; Buchan, N. I.; Larsen, C. A.; Stringfellow, G. B. *J. Cryst. Growth* **1989**, *96*, 906.

(25) Jacko, M. G.; Price, S. J. W. *Can. J. Chem.* **1964**, *42*, 1198.

Table I. Bond Strengths for As and Sb Compounds

	D_1		D_{av}^e	
	H	CH$_3$	H	CH$_3$
As	>63^a	63^c	70.5	55
Sb	≪56^b	56^d	61	51

^{a} Lum, R. M.; Klingert, J. K. *J. Appl. Phys.* **1989**, *66*, 3820. ^{b} Estimate on the basis of relative stability (see text). ^{c} Price, S. J. W.; Richard, J. P. *Can. J. Chem.* **1970**, *48*, 3209. ^{d} Price, S. J. W.; Richard, J. P. *Can. J. Chem.* **1972**, *50*, 966. ^{e} Skinner, H. A. *Adv. Organomet. Chem.* **1964**, *2*, 49.

Sb and L = H or Me. D_{av} is derived from the heat of formation; the table shows that AsH$_3$ is somewhat more stable relative to the trimethyl analogue than is SbH$_3$. Comparable information is not available for the strength of the first bond, which is often quite different from the average. The values given for D_1 of the hydrides are based on relative decomposition temperatures,[26] which imply that the first As–H bond is stronger than the corresponding As–CH$_3$ bond. For Sb the opposite is true. The extreme weakness of the Sb–H bond is demonstrated by the fact that SbH$_3$ decomposes at temperatures only slightly above room temperature.[27] (CH$_3$)$_2$SbH, the expected product of TMSb hydrogenolysis, must be kept below −78 °C to prevent decomposition.[28] In summary, hydrogenolysis is not thermodynamically favorable for TMSb while for TMAs it is more likely.

For TMIn–TMSb mixtures, the product and pyrolysis data strongly imply only indirect influences of the two components on one another. Thus formation of a Lewis acid–base adduct is not indicated. The In–Sb bond in such a molecule would be weak, because of the large atomic radii of both central atoms.[29] However, several TMIn:SbR$_3$ combinations have been reported to give adducts. Harrison and Tomkins[30] found that mixtures of TMIn vapors with those of SbH$_3$ reacted at room temperature to give CH$_4$ and an orange solid that turned gray at 150–160 °C. The pressure of SbH$_3$ was 2 Torr. TMIn and TMSb gave a liquid at room temperature, which vaporized at 65 °C. As the temperature was increased to 100 °C the quotient P/T remained constant, implying that the adduct was completely dissociated upon initial vaporization. No decomposition occurred as a result of this heating. Finally, Nemirovskii et al.[31] reported that TMIn–Sb(C$_2$H$_5$)$_3$ mixtures led to deposits on the reactor walls below 10 °C but

not above 50 °C. This last result is significant because their apparatus was a typical OMVPE growth reactor. Of the three combinations described above, only TMIn–SbH$_3$ showed any signs of decomposition. Even for that system, the results could be explained in terms of independent decomposition of SbH$_3$ to give H atoms which subsequently attack the TMIn. It can be concluded from the results described above that adduct reactions may be important in some cases, but not under the temperature and concentration conditions used in our studies or those normally encountered in OMVPE growth.

Summary

The pyrolysis of TMSb is governed by gas-phase free-radical processes. In an inert He atmosphere, CH$_3$ radicals are produced by homolytic fission. The CH$_3$ groups interact to give the products C$_2$H$_6$, C$_3$H$_8$, and CH$_4$. Another possible reaction is recombination with (CH$_3$)$_2$Sb, thereby retarding the net pyrolysis rate. The results of adding a free radical source (azomethane) and a scavenger (toluene) support the mechanism. The TMSb pyrolysis rate is decreased by the former and increased by the latter.[12]

The pyrolysis rate is greatly enhanced when He is replaced by either H$_2$ or D$_2$. In D$_2$ the main product is CH$_3$D. No (CH$_3$)$_2$SbD was found, so hydrogenolysis apparently does not occur. This is consistent with expectations from thermodynamics since the Sb–H bond is weak. When toluene was added, small amounts of HD and C$_7$H$_7$D were found, indicating the existence of atomic D. The production of these deuterated species was accompanied by a slight increase in the decomposition temperature. This suggests that the increased pyrolysis in H$_2$ or D$_2$ is due to attack on the parent TMSb by H or D atoms.

The results of adding TMIn are surprising. Adduct mechanisms are specifically not involved. In fact, no concerted group III/V pathway is operative. In the combined system the pyrolysis of TMSb is accelerated but that of TMIn is significantly retarded. This suggests that the main role of TMIn is to simply supply H radicals, via the interaction of CH$_3$ with the H$_2$ ambient. H atoms attack either TMIn or TMSb, thus accelerating their pyrolysis rates. TMIn and TMSb compete for the H atoms. Thus, assuming the rate of reaction with TMSb to be the more rapid at low temperatures where TMSb alone does not pyrolize, the TMIn pyrolysis causes an increase in the TMSb pyrolysis rate. The reduction in D concentration by reactions with TMSb decreases the TMIn pyrolysis rate.

Registry No. TMSb, 594-10-5; TMIn, 3385-78-2.

(26) Lum, R. M.; Klingert, J. K. *J. Appl. Phys.* **1989**, *66*, 3820.
(27) Devyatykh, G. G.; Kedyarkin, V. M.; Zorin, A. D. *Russ. J. Inorg. Chem.* **1969**, *14*, 1055.
(28) Burg, A. B.; Grant, L. R. *J. Am. Chem. Soc.* **1959**, *81*, 1.
(29) Patterson, D. B.; Carnevale, A. *J. Chem. Phys.* **1973**, *59*, 6464.
(30) Harrison, B. C.; Tomkins, E. H. *Inorg. Chem.* **1962**, *1*, 951.
(31) Nemirovskii, L. N.; Kozyrkin, B. I.; Lantsov, A. F.; Gribov, B. G.; Skvortsov, I. M.; Sredinskaya, I. A. *Dokl. Chem. (Engl. Transl.)* **1974**, *218*, 87.